Am J Transl Res 2022;14(7):4549-4561
www.ajtr.org /ISSN:1943-8141/AJTR0142840

Original Article

UBE2L3 promotes lung adenocarcinoma invasion and metastasis through the GSK-3β/Snail signaling pathway

Xingjie Ma[1], Weibo Qi[1], Fan Yang[1], Huan Pan[2]

Departments of [1]Cardiothoracic Surgery, [2]Central Laboratory, First Affiliated Hospital of Jiaxing University, Jiaxing 314001, Zhejiang, China

Received March 13, 2022; Accepted May 20, 2022; Epub July 15, 2022; Published July 30, 2022

Abstract: Lung cancer is the leading cause of cancer-related mortality, and the deaths are mostly attributed to distant metastasis. Previous studies have demonstrated that ubiquitin-conjugating enzyme E2 L3 (UBE2L3) mediates the progression of many human cancers. However, the roles and molecular mechanisms of UBE2L3 in invasion and metastasis of lung adenocarcinoma (LUAD) are yet to be fully understood. Here, we studied the expression pattern of UBE2L3 and demonstrated that it is dramatically up-regulated in LUAD tissues compared with the normal tissues, and its overexpression is positively correlated with lymph node metastasis. Moreover, the upregulation of UBEE2L3 in LUAD tissues is associated with shorter overall survival (OS). UBE2L3 silencing impairs the metastatic capacity of LUAD cells *in vitro* and *in vivo*, while its overexpression confers an opposite effect. In addition, our data showed that UBE2L3 promotes cancer cells epithelial-mesenchymal transition (EMT) and metastasis via the glycogen synthase kinase 3β (GSK-3β)/Snail axis. Besides, UBE2L3 was shown to promote ubiquitination and degradation of the GSK-3β. Immunohistochemical analysis demonstrated that UBE2L3 expression is positively correlated with Snail, but negatively correlated with GSK-3β and E-cadherin in LUAD tissues. Taken together, our findings demonstrated that UBE2L3 modulates metastasis of LUAD cells.

Keywords: Lung adenocarcinoma, metastasis, EMT, GSK-3β, Snail

Introduction

Lung cancer is the most common malignant tumor and the leading cause of cancer-related death in the world [1]. Although there are many advances in the early diagnosis and treatment of lung cancer, distant metastasis remains the main contributor to mortality in lung cancer patients [2-4]. Cancer metastasis is a complicated multistep process, which involves numerous genes and signaling pathways [5]. Therefore, there is a need to define metastasis-associated biomarkers and their mechanisms, which would guide therapeutic strategies.

Cancer metastasis is driven by the process of epithelial-to-mesenchymal transition (EMT) in which epithelial cells lose their polarity and develop mesenchymal phenotypes. This shift makes cancer cells acquire migratory and invasion properties [6]. It has been demonstrated that EMT plays a critical role in inducing cancer cell invasion and metastasis. At the early stage of metastasis, epithelial markers such as E-cadherin and ZO-1 are downregulated, while mesenchymal markers such as N-cadherin and vimentin are up-regulated [7]. This transformation is driven by EMT-inducing transcription factors such as Snail1/2, Slug1/2, and Twist1/2 [8, 9]. EMT process is regulated by many oncogenic signaling pathways, which include Wnt, NF-KB, Notch, and PI3K/AKT pathways [10]. Thus, evaluation of molecular regulatory mechanisms of EMT is essential in improving the outcome of patients with advanced lung cancer.

The ubiquitin-proteasome system (UPS) is a major protein degradation pathway, which maintains protein homeostasis in cells [11]. Briefly, protein ubiquitination is a three-step process that is mediated by E1 ubiquitin-activating enzyme, E2 ubiquitin-conjugating enzyme, and E3 ubiquitin ligase. Thereafter, the ubiquitin-tagged proteins are degraded by the ATP-dependent 26s proteasome complex. The UBE2L3 protein is a member of the E2 ubiqui-

tin-conjugating enzyme [12, 13]. Accumulating evidence indicates that aberrant UBE2L3 expression is associated with oncogenesis in many cancer types. For instance, UBE2L3 could promote cell proliferation and invasion in prostate cancer [14]. Besides, overexpression of the UBE2L3 has been shown to mediate carcinogenesis in hepatocellular carcinoma [15]. Our previous study showed that UBE2L3 mediates p27kip1 ubiquitination and degradation to promote lung cancer cell growth [16]. However, the functions and mechanisms of UBE2L3 in lung cancer metastasis remain unclear.

Here, we demonstrated that UB2L3 plays a critical role in the metastasis of LUAD cells. UB2L3 promotes cancer cell migration and invasion *in vitro* and *in vivo*. Furthermore, analysis of the molecular mechanisms revealed that UBE2L3 promotes metastasis via GSK-3β/Snail axis. In addition, the UBE2L3 protein fuels the ubiquitination and degradation of GSK-3β. On the other hand, Snail knockdown largely attenuated the UBE2L3-induced migration and invasion. These findings demonstrate robustly that UBE2L3 induces the EMT process which drives cancer metastasis.

Materials and methods

Specimens and immunohistochemical (IHC) assays

Tissue specimens were collected from LUAD patients who underwent surgical resection in the First Hospital of Jiaxing. The specimens were pathologically diagnosed with LUAD. None of the patients received immunotherapy, chemotherapy, or radiation before surgery. This study was approved by the Research Ethics Committee of the First Hospital of Jiaxing (LS2019-125). Clinicopathological data were obtained from medical records.

Immunohistochemistry staining (IHC) was performed according to the protocol. Briefly, each tissue section was stained with specific antibodies according to the manufacturer's instructions. The intensity score was graded as follows: 0 (negative staining); 1 (week staining); 2 (moderate staining) and 3 (strong staining); while the proportion of positive cells was scored as 0-100%. The histochemical score (H-score) was calculated by multiplying the percentage of positive cells with the staining intensity grade. The cut-off value of the UBE2L3 expression was used as the median H-score.

Cell culture

The human LUAD cell lines A549 and H1299 were obtained from the Cell Bank of the Chinese Academy of Sciences (Shanghai, China). The cells were cultured in RPMI-1640 medium supplemented with 10% fetal bovine serum (FBS), penicillin (10^7 U/L), and streptomycin (10 mg/L) at 37°C in a 5% CO_2 atmosphere.

Transfection of plasmids and shRNAs

UBE2L3-expressing plasmid and control plasmid were purchased from Cyagen Biosciences (USA). UBE2L3 shRNA and the negative control shRNAs were obtained from GenePharm (China). The A549 and H1299 cells were seeded into 6-well plates (3×10^7 cells/well) and cultured in RPMI-1640 medium, supplemented with 10% FBS without antibiotics for 24 h prior to transfection. When the cells were at 60-70% confluency, they were transfected with 4 μg of the plasmids using Lipofectamine 3000 (Invitrogen, USA) according to the manufacturer's instructions.

RNA extraction and real-time-PCR

Total RNA was extracted using TRIzol reagent (Invitrogen, USA), following the manufacturer's instructions. The first-strand cDNA synthesis was performed using PrimeScript Reverse Transcriptase (TaKaRa, Japan) while quantitative real-time polymerase chain reaction (qRT-PCR) was conducted using SYBR Green Supermix (Bio-Rad, USA), with 1 μl cDNA template. Relative expression of the protein was calculated using the comparative ΔΔCT method, and GAPDH was used as an internal reference gene. The reactions were performed in triplicate, and the results were presented as mean ± SD.

Immunoblotting and co-immunoprecipitation assay

Cells were lysed, and then total protein was extracted using RIPA lysis buffer. The total protein concentrations were determined by the BCA protein assay kit (Pierce, USA), following the manufacturer's instructions. The protein lysates were resolved in 10% SDS-PAGE gels

and then transferred onto PVDF membranes. The blots were blocked and then incubated with primary antibodies overnight at 4°C. Thereafter, the blots were washed and incubated with secondary antibodies for 2 h at room temperature. After 3 washes in TBST, the blots were developed with enhanced chemiluminescent (ECL) detection kit and then immunoreactive bands were analyzed.

For co-immunoprecipitation (co-IP) assays, the whole-cell lysates were incubated with the desired antibodies. The target protein was then pulled down with protein-A/G magnetic beads (Millipore, USA) and subjected to immunoblotting analysis, following the manufacturer's instructions.

Cell wound healing, migration, and invasion assays

Cell wound healing assay was used to evaluate the capability of cell migration. Briefly, an incision was made in the central area of each well in the 6-well plates to create an artificial wound. Images of the wound area were captured at 0 and 24 h after injury. Wound closure was quantified using Adobe Photoshop software and the percentage was calculated relative to the initial time point.

Transwell assays were performed using Transwell chambers (8 μm pores, Corning, USA), with or without pre-coated Matrigel (BD Biosciences, USA). Cells, at a density of 5×10^4 per well, were seeded in the upper chamber without serum. The lower chamber was filled with a medium containing 10% fetal bovine serum (FBS). After further incubation, the cells that had migrated or invaded the other side of the membrane were fixed with 4% paraformaldehyde for 20 min and then stained with 0.1% crystal violet for 30 min. Five fields in each well were photographed.

Ubiquitination and protein stability assay

For the ubiquitination assay, the cells were harvested 48 h after transfection with the indicated plasmids. Cell lysates were immunoprecipitated using respective antibodies, followed by immunoblotting with anti-ubiquitin antibodies.

The stability of the GSK-3β protein was determined by the cycloheximide chase (CHX) assay. Cells were treated with 100 μg/ml cycloheximide (Sigma, USA) and then harvested at the indicated times. Thereafter, the cell lysate was obtained and analyzed by immunoblotting.

In vivo metastasis assay

All animal procedures and experimental protocols were approved by the Institutional Animal Care and Use Committee of the First Affiliated Hospital of Jiaxing University. BALB/c nude mice (aged 4 weeks) were purchased from Zhejiang Vital River Laboratory and maintained in a specific pathogen-free (SPF) environment. Cells were harvested and suspended in PBS. For tail vein injection assay, 100 μl of cell suspension (1×10^6 cells) was injected into the lateral tail vein of nude mice. The mice were sacrificed 4 weeks post-injection and then lung metastasis nodules were counted. The lungs were resected, fixed in 4% polyoxymethylene, and examined by hematoxylin and eosin (HE) staining.

Statistical analysis

Statistical analyses were performed by SPSS version 25.0 (IBM, USA). Results were presented as mean ± SD (standard deviation). Statistical comparisons were performed by a two-tailed unpaired Student's *t*-test. Clinical correlation of the UBE2L3 staining and lymph node invasion was performed using the chi-square test. In addition, the chi-square test was used to analyze the relationship between UBE2L3 and Snail, GSK-3β, or E-cadherin. A $P<0.05$ was considered statistically significant.

Results

UBE2L3 overexpression predicts metastasis and poor prognosis in lung adenocarcinoma

Our previous study demonstrated that UBE2L3 is highly expressed in non-small cell lung cancer (NSCLC), and the high UBE2L3 expression is associated with poor overall survival (OS) in patients with NSCLC. In the current study, we explored whether high expression of UBE2L3 is associated with greater metastatic potential in LUAD. First, we analyzed the UBE2L3 expression and clinical data from the TCGA-LUAD dataset. Patients were divided into high and low expression groups based on the median

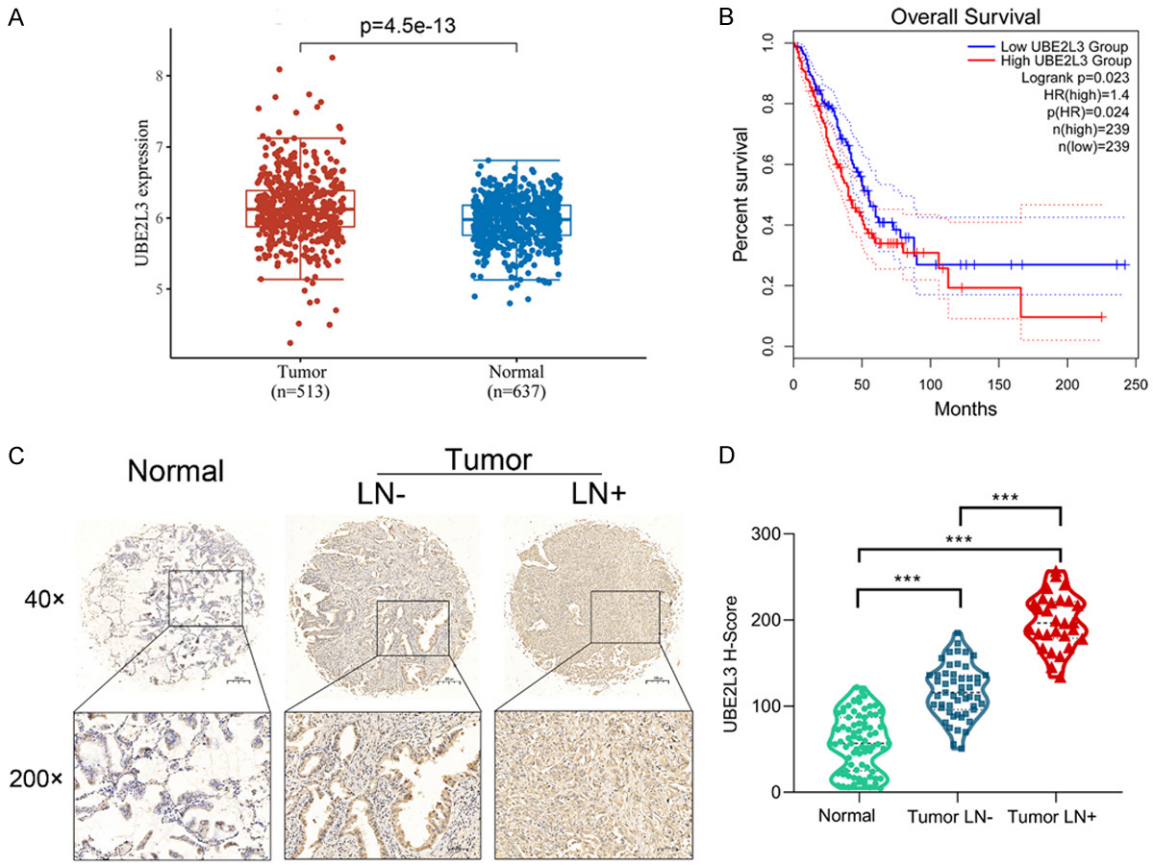

Figure 1. High UBE2L3 expression correlates with metastasis and poor prognosis in LUAD. The expression profiling and survival analysis in the TCGA-LUAD dataset. A. Box plot analysis of the UBE2L3 mRNA expression in LUAD tissues and normal tissues from the TCGA. B. Kaplan-Meier analysis of the overall survival in LUAD patients based on the expression of UBE2L3. C. Representative immunohistochemistry (IHC) images of UBE2L3 expression in the normal tissues and LUAD tissues with or without lymph node metastasis. Magnification: 40× (scar bar =200 μm) and 200× (scar bar =50 μm). D. H-score was calculated by multiplying the intensity score and the percentage of positive cells (range, 0-300). UBE2L3 was significantly overexpressed in LUAD tissues with lymph node metastasis compared to the LUAD tissues without lymph node metastasis. LN-, lymph node metastasis negative; LN+, lymph node metastasis positive; ***P<0.001.

UBE2L3 expression. Our data showed that compared with the normal tissues, UBE2L3 was significantly up-regulated in LUAD tissues (**Figure 1A**, P<0.001), and was associated with poor OS (**Figure 1B**, P=0.024). We then employed IHC to examine the expression of UBE2L3 in our own patients' cohort. Strikingly, our results demonstrated there was increased expression of UBE2L3, which was proportional to the cancer progression from normal tissues to the tumor without lymph node metastasis and to the tumor with lymph node metastasis (**Figure 1C**, **1D**). The H-score was significantly higher in the LUAD tissues with lymph node metastasis (194.4±31.2) than that in tissues without lymph node metastasis (117±30.4; P<0.001). Taken together, these data suggested that UBE2L3 was notably up-regulated in LUAD, which may be a prognostic biomarker for metastasis.

Deletion of UBE2L3 suppresses LUAD metastasis in vitro and in vivo

To investigate the role of UBE2L3 in invasion and metastasis of LUAD cells, we established stable UBE2L3 knockdown LUAD cells (A549/shUBE2L3 and H1299/shUBE2L3), which was confirmed by immunoblotting (**Figure 2A**). Wound healing assays demonstrated that UBE2L3 knockdown suppressed migratory abilities in both A549 cells (55.0±5.3 vs. 30.6±4.7, P<0.001) and H1299 cells (36.2±4.6 vs. 18.8±4.1, P<0.001) (**Figure 2B**). More-

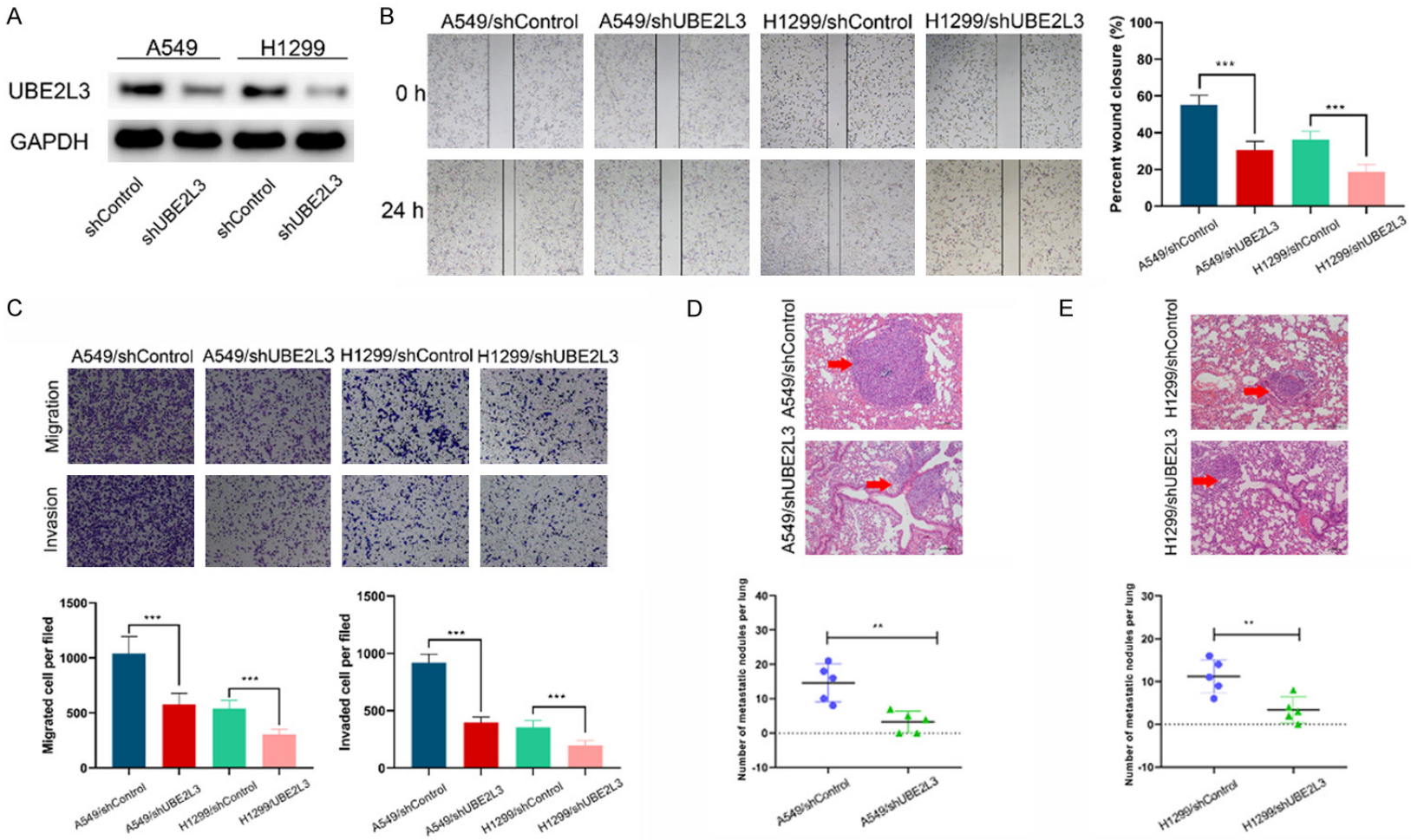

Figure 2. Depletion of UBE2L3 inhibits metastasis of LUAD cells. A. Immunoblotting analyses were performed to determine the expression of UBE2L3 in LUAD cells. B. Representative images of wound healing assays and the percentage of wound closure. Magnification: 40× (scar bar =200 μm). C. The effect of UBE2L3 konck-down on the migration and invasion of LUAD cells was assessed using Transwell assays. Magnification: 100× (scar bar =100 μm). D, E. Representative HE staining of lung metastasis after the injection of cancer cells into BALB/c mice via tail vein. Magnification: 100× (scar bar =100 μm). Quantification of lung metastasis (n=5 mice per group). ***P<0.001; **P<0.001.

over, UBE2L3 silencing significantly inhibited migration and invasion in A549 cells (P< 0.001) and H1299 cells (P<0.001) (**Figure 2C**). In addition, we generated pulmonary metastasis models by injecting A549/shUBE2L3, H1299/shUBE2L3, and the control cells into nude mice via tail veins. Our data revealed that UBE2L3 knockdown notably decreased the number of lung metastatic nodules (**Figure 2D**, **2E**).

Overexpression of UBE2L3 promotes metastasis

To determine whether UBE2L3 overexpression could exert an opposite effect to UBE2L3 knockdown, we established stable UBE2L3 overexpression cells (A549/UBE2L3 and H1299/UBE2L3) as shown in **Figure 3A**. Our analysis demonstrated that UBE2L3 overexpression significantly enhanced migration and invasion of LUAD cells (**Figure 3B**, **3C**). For analysis of experimental lung metastasis, A549/UBE2L3 and H1299/UBE2L3 cells were intravenously injected. The data showed that UBE2L3 upregulation significantly increased lung metastasis of both A549 and H1299 cells (**Figure 3D**, **3E**). These results revealed that UBE2L3 was associated with invasion and metastasis in LUAD cells.

UBE2L3 promotes GSK-3β ubiquitination and degradation

Since previous studies reported that UBE2L3 could degrade GSK-3β in hepatocellular carcinoma, we investigated whether this phenomenon persisted in LUAD. Our immunoblot analyses demonstrated that GSK-3β protein expression was negatively associated with UBE2L3, while GSK-3β mRNA expression remained unchanged (**Figure 4A**). We then examined the GSK-3β protein half-life by treating the H1299/UBE2L3 cells and the control cells with cycloheximide (CHX) to block new protein synthesis, and then the cells were harvested at the indicated time points. The CHX assays showed that there was a higher rate of GSK-3β degradation in H1299/UBE2L3 cells (**Figure 4B**).

We co-transfected myc-UBE2L3 and Flag-GSK-3β to 293T cells and performed co-IP assays. The co-IP analyses demonstrated that exogenously expressed myc-UBE2L3 bound co-expressed Flag-GSK-3β and vice versa (**Figure 4C**, **4D**). Thereafter, co-IP assays were performed to confirm the interaction between endogenous UBE2L3 and GSK-3β in H1299 and A549 cells (**Figure 4E**, **4F**). The results showed that endogenous UBE2L3 was co-immunoprecipitated by endogenous GSK-3β. Taken together, these results demonstrated that UBE2L3 interacts with both exogenous and endogenous GSK-3β in cells.

H1299/UBE2L3, A549/UBE2L3 and the control cells were harvested after treatment with 20 μM MG132 for 4 hours. The cell lysates were immunoprecipitated with anti-GSK-3β antibodies, and then ubiquitination was analyzed with anti-ubiqutin antibodies. We observed that UBE2L3 overexpression dramatically promoted the ubiquitination of GSK-3β in H1299 and A549 cells (**Figure 4G**, **4H**). Collectively, these findings suggested that UBE2L3 regulates the degradation of GSK-3β protein via ubiquitination.

UBE2L3 up-regulates Snail expression in GSK-3β dependent manners

To gain insights into the molecular mechanism of UBE2L3 in the modulation of metastasis in LUAD cells, we examined the expression of the key EMT markers. As shown in **Figure 5A**, UBE2L3 knockdown increased the expression of E-cadherin and decreased the expression of Snail. In contrast, UBE2L3 overexpression suppressed the expression of E-cadherin and increased the expression of Snail. Therefore, UBE2L3 induced EMT progression in LUAD cells. Previous studies revealed that GSK-3β could mediate the stabilization of Snail. Thus, we investigated whether the GSK-3β/Snail axis is involved in the metastasis of LUAD cells. A549/shUBE2L3 and H1299/shUBE2L3 cells were treated with a GSK-3β inhibitor (CHIR 99021) before analysis. The results showed that the GSK-3β inhibitor blocked the upregulation of E-cadherin and downregulation of Snail, which were induced by UBE2L3 knockdown (**Figure 5B**). Taken together, these findings demonstrated that UBE2L3 elevates Snail levels and promotes EMT in a GSK-3β dependent manner.

UBE2L3 depends on elevated Snail to enhance LUAD cell invasion and metastasis

To further explore the molecular pathways that drive the UBE2L3 mechanisms, Snail was kn-

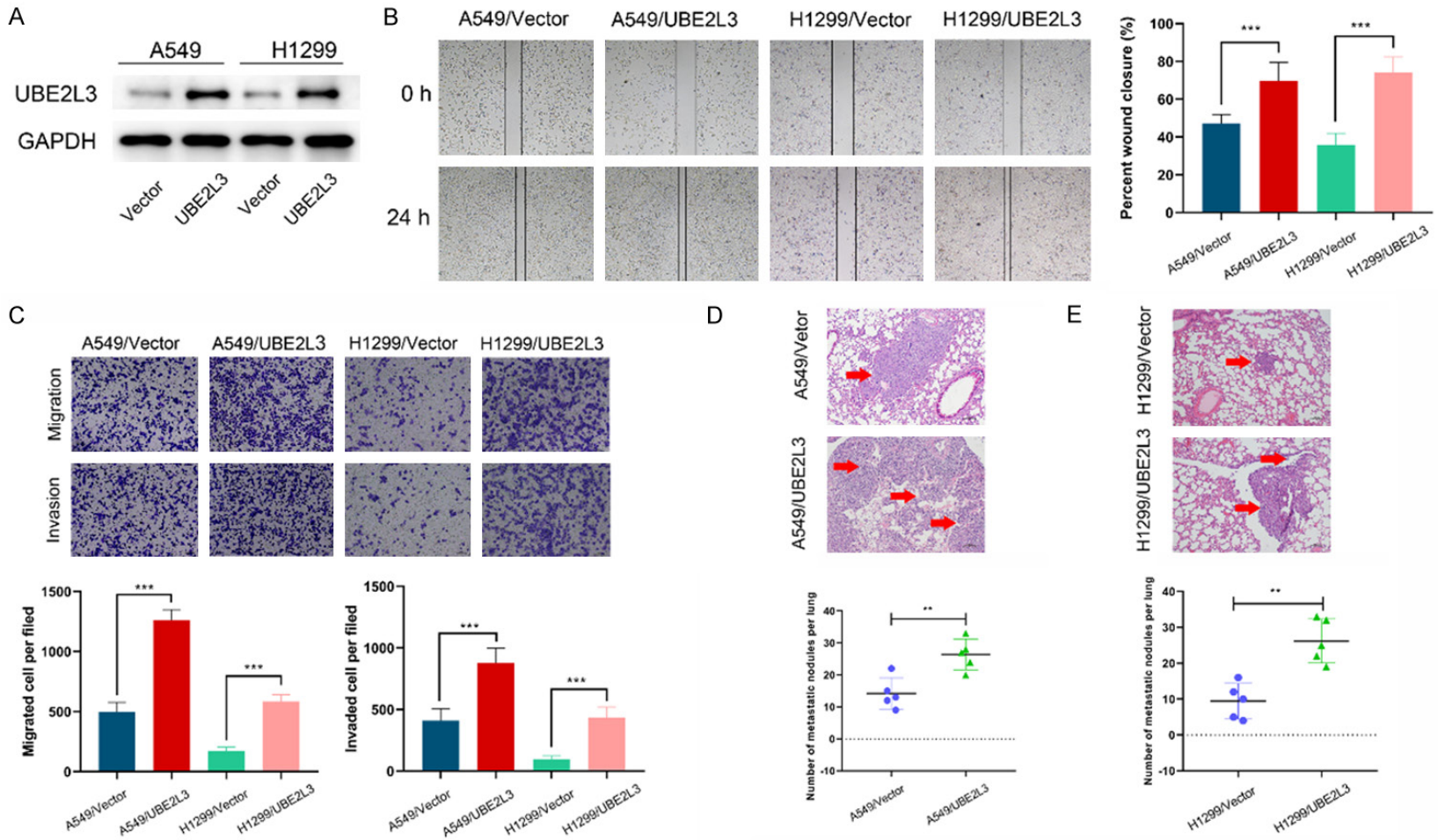

Figure 3. Overexpression of UBE2L3 promotes tumor cell metastasis. A. Immunoblotting analyses were performed to determine the expression of UBE2L3 in LUAD cells. B. Representative images of wound healing assays and the percentage of wound closure. Magnification: 40× (scar bar =200 μm). C. The effect of UBE2L3 overexpression on the migration and invasion of LUAD cells was assessed using Transwell assays. Magnification: 100× (scar bar =100 μm). D, E. Representative HE staining of lung metastasis after the injection of cancer cells into BALB/c mice via tail vein. Magnification: 100× (scar bar =100 μm). The quantification of lung metastasis (n=5 mice per group). ***P<0.001; **P<0.001.

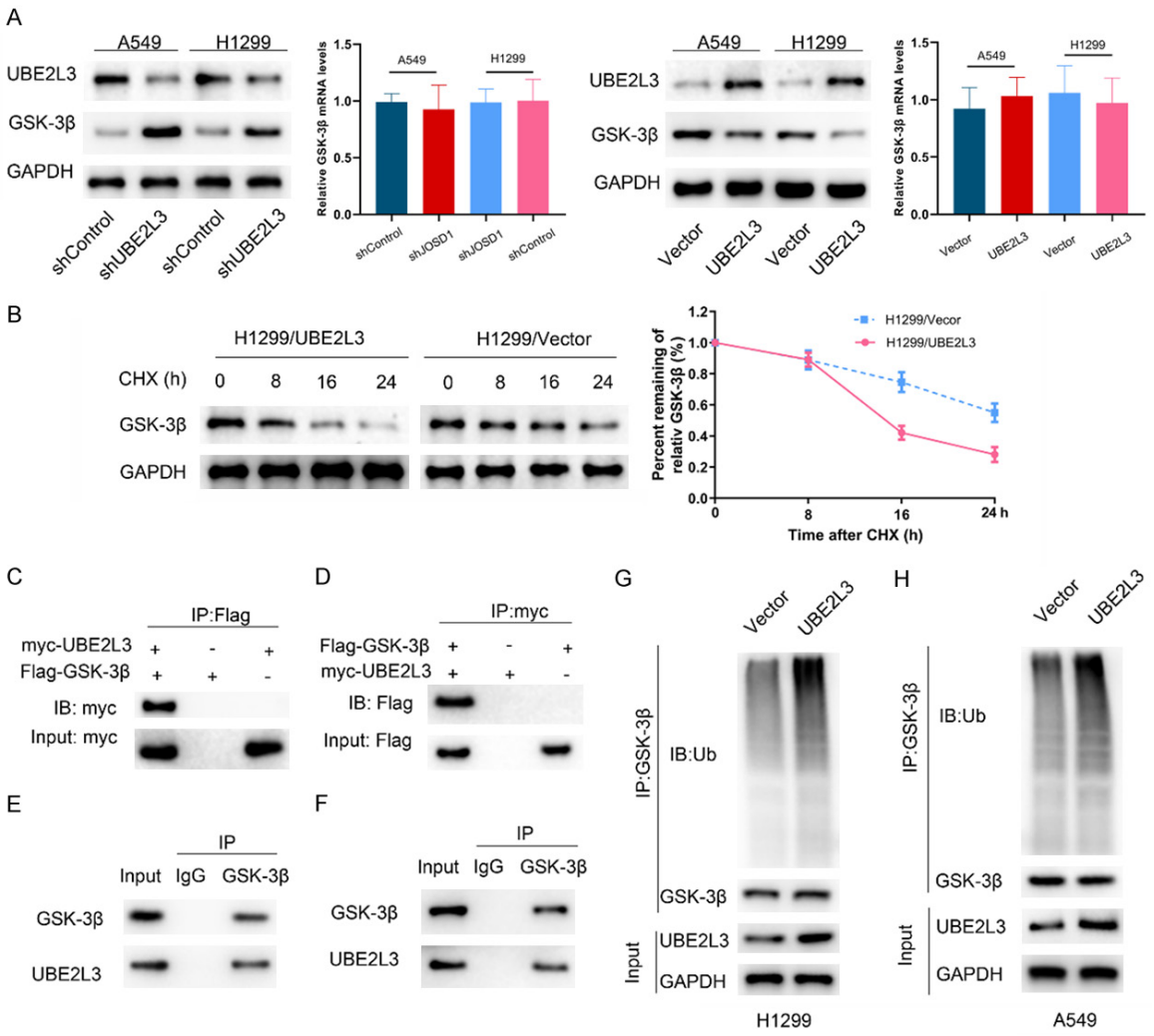

Figure 4. UBE2L3 interacts with and ubiquitinates GSK-3β. (A) GSK-3β levels were determined through immunoblotting and qRT-PCR. (B) H1299/UBE2L3 and the control cells were treated with 100 μg/ml CHX. The cells were harvested and subjected to immunoblotting at different times. Quantification of the UBE2L3 levels, which were normalized to GAPDH levels at 0 h. (C, D) 293T cells were co-transfected with Flag-GSK-3β and myc-UBE2L3 plasmids. Reciprocal co-immunoprecipitation of myc-UBE2L3 and Flag-GSK-3β in co-transfected 293T cells. Endogenous UBE2L3 interacted with GSK-3β in H1299 cells (E) and A549 cells (F). Cells were treated with 20 μM MG132 for 4 h. The cells were harvested and subjected to immunoblotting analyses with anti-Ubiquitin antibodies. UBE2L3 overexpression dramatically promoted the ubiquitination of GSK-3β in H1299 cells (G) and A549 cells (H).

ocked down in both the UBE2L3 overexpressing cells (H1299/UBE2L3 cells) and the control cells using specific shRNAs. The knockdown efficiency was assessed by immunoblot assays as shown in **Figure 6A**. The wound healing and Transwell assays showed that Snail knockdown significantly impaired UBE2L3-induced cell migration and invasion (**Figure 6B**, **6C**). Besides, Snail silencing significantly inhibited UBE2L3-induced lung metastasis *in vivo* (**Figure 6D**). These results revealed that UBE2L3-enhanced tumor invasion and metastasis largely depended on elevated Snail.

Clinical significance of UBE2L3/GSK-3β/Snail crosstalk in the LUAD samples

To evaluate potential clinical significance of the UBE2L3/GSK-3β/Snail crosstalk in LUAD progression, we analyzed the expression of UBE2L3, GSK-3β, Snail, and E-cadherin using IHC. The clinical tissue samples were divided into UBE2L3-high and UBE2L3-low groups based on the median H-score (145.9). Specimens with a score <145.9 were classified as low UBE2L3, and those with a score ≥145.9 were classified as high UBE2L3. As shown in

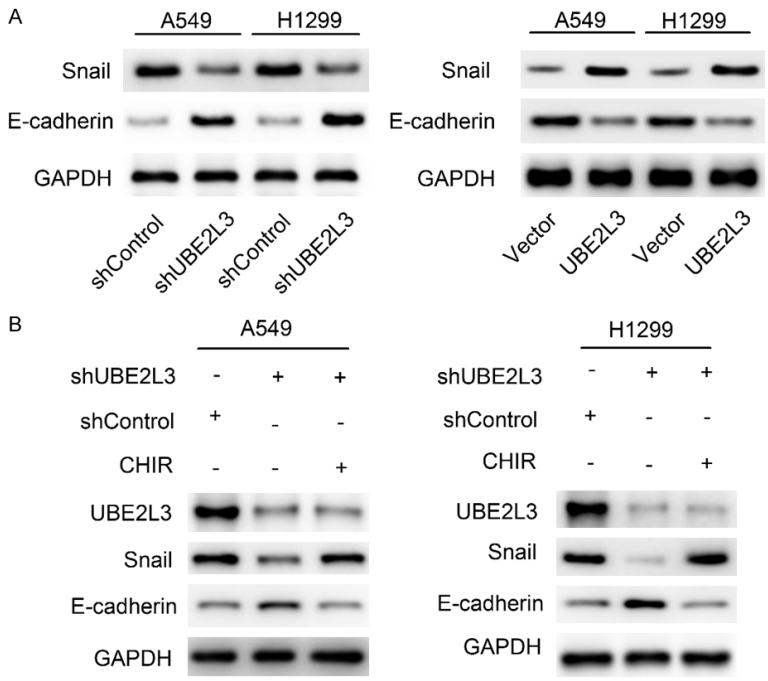

Figure 5. UBE2L3 up-regulates Snail expression in a GSK-3β dependent manner. A. The effect of UBE2L3 expression on the EMT markers (Snail and E-cadherin) was determined by immunoblotting. B. Immunoblotting analyses were performed to assess the effect of the GSK-3β inhibitor (CHIR 99021) on EMT makers.

Figure 7A, **7B**, UBE2L3 expression was positively associated with Snail ($P<0.01$), but negatively correlated with GSK-3β ($P<0.01$) and E-cadherin ($P<0.05$). Collectively, these findings suggested that UBE2L3/GSK-3β/Snail crosstalk fuels LUAD progression, and high expression of UBE2L3 predicts a higher risk of metastasis. A schematic diagram of this study is presented in **Figure 7C**.

Discussion

Although great progress has been made in comprehensive treatment over decades, lung cancer remains the leading cause of cancer-related deaths worldwide [17]. Lung adenocarcinoma (LUAD) is the most common pathological type of lung cancer, and it is characterized by a high rate of invasion and metastasis [18]. Cancer metastasis and recurrence remain as major challenges in the treatment and clinical management of LUAD patients. Indeed, cancer metastasis is the main cause of mortality in LUAD patients. In this study, we revealed a novel role of UBE2L3 in the metastasis of LUAD cells.

Our previous studies demonstrated that UBE2L3 could promote cancer cell growth by ubiquitination and degradation of p27kip1 in non-small cell lung cancer (NSCLC) [16]. In this study, we evaluated the roles of UBE2L3 in cancer metastasis. Our data showed that UBE2L3 was dramatically up-regulated along with the LUAD progression, from adjacent normal tissues to primary tumor and then to tumor with metastasis. These findings were further validated by analyses of the TCGA-LUAD dataset. Besides, high expression of UBE2L3 was associated with poor prognosis. To investigate the effect of UBE2L3 on LUAD cell invasion and metastasis, UBE2L3 expression was stably silenced or overexpressed in A549 and H1299 cells. UBE2L3 knockdown significantly inhibited cell invasion and metastasis, while UBE2L3 overexpression had an opposite effect. Thus, UBE2L3 may be playing an essential role in the progression of LUAD cell metastasis.

Previous data demonstrated that EMT is a critical step in the invasion and metastasis of LUAD [19]. EMT is a complex process in which cells lose epithelial features, such as cellular junctions and polarity, and acquire characteristics of invasive mesenchymal cells [20]. Despite the fact that signaling pathways are rather complicated, the primary hall marker of EMT in lung cancer is loss of expression of E-cadherin [21]. E-cadherin is a cell-cell adhesion molecule and is a repressor of invasion and metastasis. Snail is a vital transition factor that functions as a repressor of E-cadherin expression and an inducer of EMT in various human tumors [22, 23]. Our analysis demonstrated that UBE2L3 overexpression decreased the expression of epithelial markers (E-cadherin) but enhanced the expression of mesenchymal markers (Snail). These findings suggested that UBE2L3 promotes migration and invasion of LUAD cells via the EMT pathway.

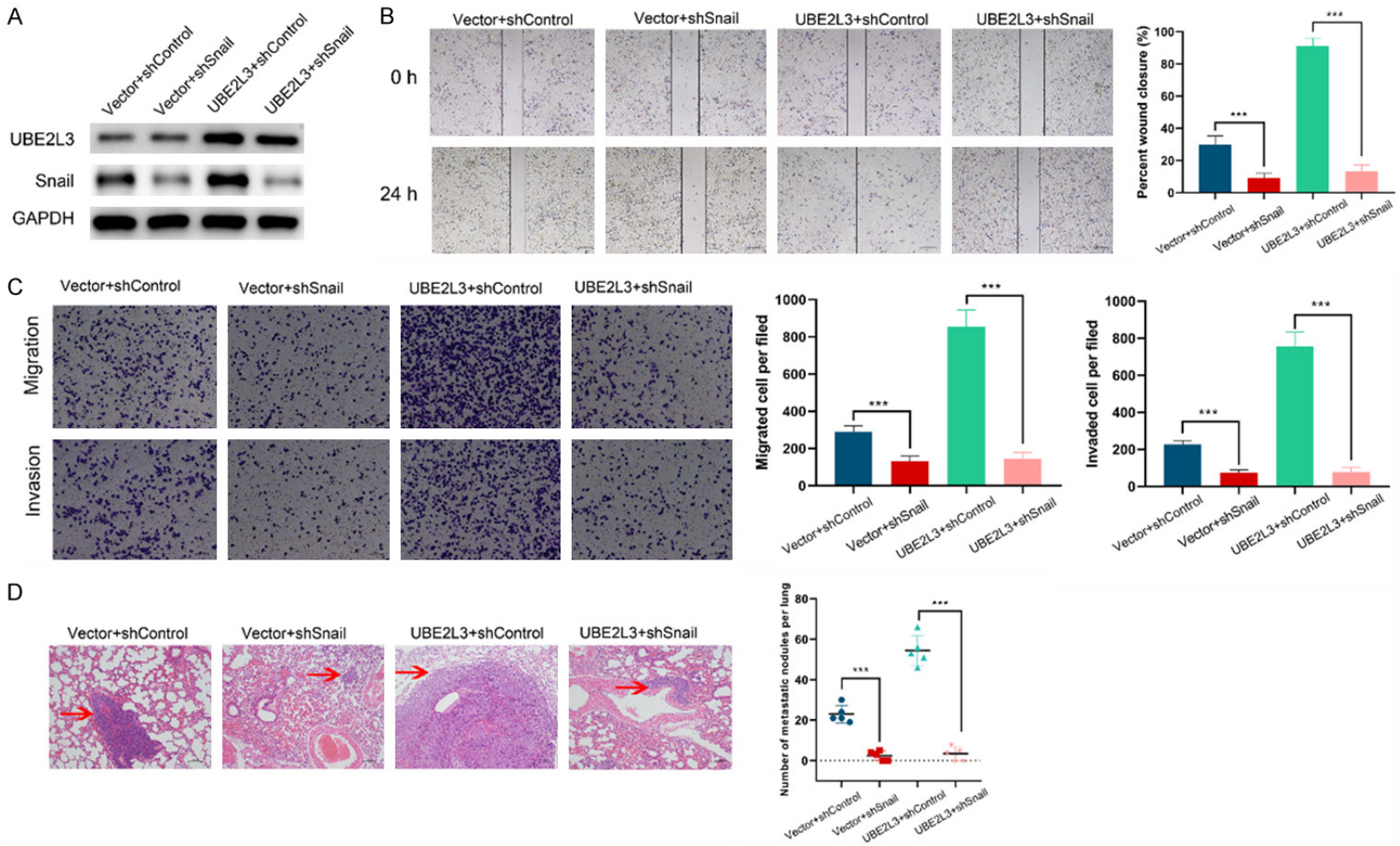

Figure 6. UBE2L3 is dependent on elevated Snail to enhance migration and invasion of LUAD cells. A. The efficiency of Snail knockdown in H1299 cells was assessed by immunoblotting. B. Representative images of wound healing assays and the percentage of wound closure were quantified. H1299 cells were co-transfected with the UBE2L3 expression vector and Snail shRNA or control shRNA. Snail knockdown suppressed the cell migration induced by UBE2L3. Magnification: 40× (scar bar =200 μm). C. Cells were analyzed by Transwell assays. Magnification: 100× (scar bar =100 μm). D. Knockdown of Snail inhibited the lung metastasis induced by UBE2L3 *in vivo*. Representative HE staining of lung metastasis after injection of cancer cells into BALB/c mice via the tail vein. Magnification: 100× (scar bar =100 μm). Quantification of lung metastasis by section of the whole lung (n=5 mice per group). ***P<0.001.

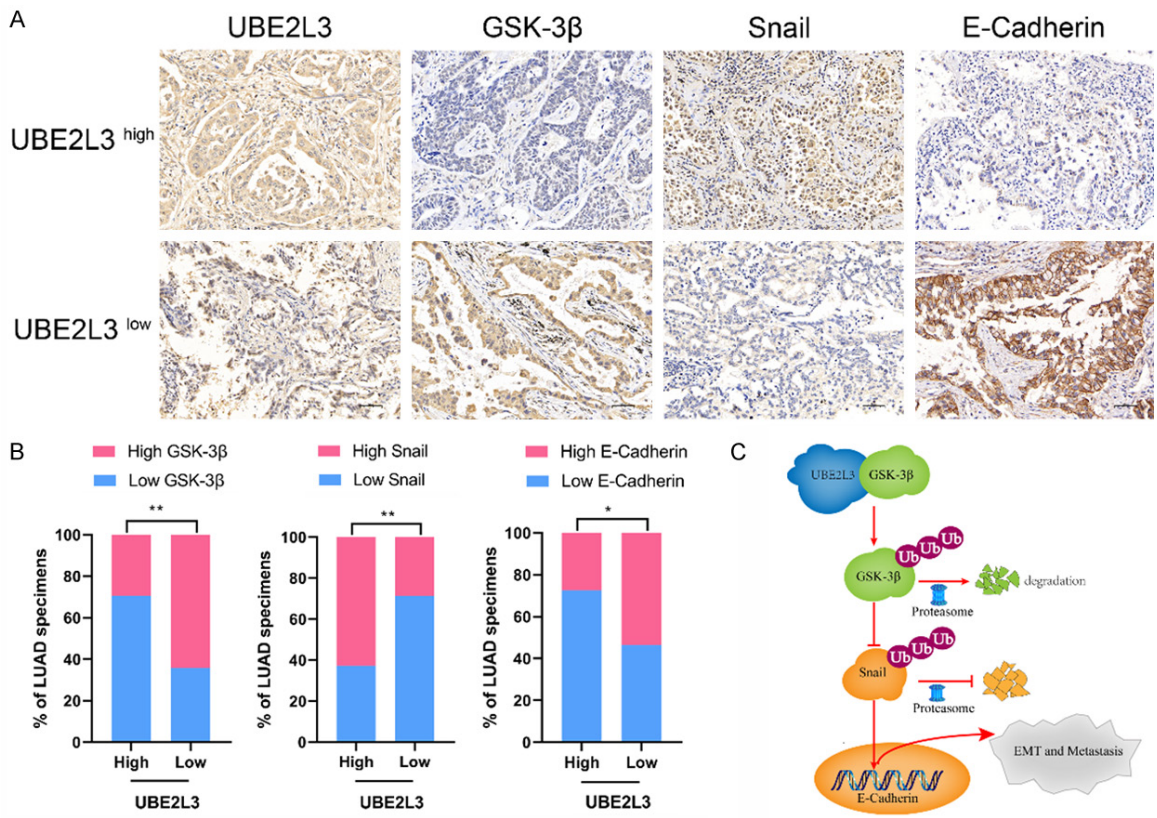

Figure 7. Clinical significance of UBE2L3/GSK-3β/Snail crosstalk in LUAD and schematic diagram. A. Representative immunohistochemical images of LUAD specimens stained with UBE2L3, GSK-3β, Snail, or E-cadherin antibodies. Magnification: 200× (scar bar =50 μm). B. Quantification of the immunohistochemistry analyses. Chi-square test was used to analyze the relationship between UBE2L3 and Snail, GSK-3β, or E-cadherin. $^{**}P<0.01$; $^{*}P<0.05$. C. The schematic diagram shows that UBE2L3 promotes LUAD cell migration and invasion by inducing EMT through the GSK-3β/Snail axis.

GSK-3β is a conserved serine/threonine kinase which plays pivotal roles in various biological events such as metastasis, proliferation, cell differentiation, autophagy, and DNA repair [24]. The activation of GSK-3β is regulated by phosphorylation, and phosphorylation of the N-terminal S9 by upstream kinases suppresses the kinase activity of GSK-3β. Increasing evidence shows that GSK-3β is involved in the onset and progression of many tumors, which include pancreatic cancer, gastric cancer, colorectal cancer, and breast cancer [25, 26]. Previous studies have shown that GSK-3β aberrant expression predicts poor OS in non-small cell lung cancer [27, 28]. In the current study, we showed that UBE2L3 prompted the ubiquitylation and degradation of GSK-3β in LUAD cells, which was consistent with a previous study [29]. Interestingly, our data showed that GSK-3β acts as an essential regulator of Snail. Activated GSK-3β can phosphorylate Snail, which induces the degradation of Snail. Briefly, Snail is phosphorylated at serine residues by GSK-3β, which is then recognized by β-TrCP1 ubiquitin ligase to accelerate its ubiquitination-mediated degradation [30, 31].

Given that GSK-3β provides a mechanistic link between UBE2L3 and Snail, we assessed whether UBE2L3 promotes cancer metastasis via the GSK-3β/Snail axis. First, we showed that the GSK-3β inhibitor largely rescued cancer cells from migration and invasion inhibition induced by UBE2L3 knockdown. Second, Snail knockdown in UBE2L3-overexpressing H1299 cells significantly impaired UBE2L3-induced metastasis *in vitro* and *in vivo*. These findings demonstrated that UBE2L3 promoted EMT and metastasis via the GSK-3β/Snail signaling pathway.

Taken together, our findings demonstrated that UBE2L3 promotes metastasis in LUAD cells. We also showed that UBE2L3 up-regulates the

expression of Snail in a GSK-3β dependent manner. The accumulated Snail induces the progression of EMT, which results in cancer metastasis. Our results highlight the roles of UBE2L3 and demonstrate that it is a potential target for drug development.

Acknowledgements

This study was supported by the Natural Science Foundation of Zhejiang Province (LQ20H16-0058), the Jiaxing Key Laboratory of Precision Treatment for Lung Cancer, and Jiaxing Science and Technology Bureau (2019AD32250).

Disclosure of conflict of interest

None.

Address correspondence to: Dr. Huan Pan, Department of Central Laboratory, First Affiliated Hospital of Jiaxing University, Jiaxing 314001, Zhejiang, China. Tel: +86-13819397202; E-mail: panhuan_xue@163.com

References

[1] Sung H, Ferlay J, Siegel RL, Laversanne M, Soerjomataram I, Jemal A and Bray F. Global cancer statistics 2020: GLOBOCAN estimates of incidence and mortality worldwide for 36 cancers in 185 countries. CA Cancer J Clin 2021; 71: 209-249.

[2] Ruiz-Cordero R and Devine WP. Targeted therapy and checkpoint immunotherapy in lung cancer. Surg Pathol Clin 2020; 13: 17-33.

[3] Melosky B, Wheatley-Price P, Juergens RA, Sacher A, Leighl NB, Tsao MS, Cheema P, Snow S, Liu G, Card PB and Chu Q. The rapidly evolving landscape of novel targeted therapies in advanced non-small cell lung cancer. Lung Cancer 2021; 160: 136-151.

[4] Simeone JC, Nordstrom BL, Patel K and Klein AB. Treatment patterns and overall survival in metastatic non-small-cell lung cancer in a real-world, US setting. Future Oncol 2019; 15: 3491-3502.

[5] Tan Q, Cui J, Huang J, Ding ZP, Lin H, Niu XM, Li ZM, Wang G, Luo QQ and Lu S. Genomic alteration during metastasis of lung adenocarcinoma. Cell Physiol Biochem 2016; 38: 469-486.

[6] Mi L, Zhu F, Yang X, Lu J, Zheng Y, Zhao Q, Wen X, Lu A, Wang M, Zheng M, Ji J and Sun J. The metastatic suppressor NDRG1 inhibits EMT, migration and invasion through interaction and promotion of caveolin-1 ubiquitylation in human colorectal cancer cells. Oncogene 2017; 36: 4323-4335.

[7] Nieszporek A, Skrzypek K, Adamek G and Majka M. Molecular mechanisms of epithelial to mesenchymal transition in tumor metastasis. Acta Biochim Pol 2019; 66: 509-520.

[8] Shih JY and Yang PC. The EMT regulator slug and lung carcinogenesis. Carcinogenesis 2011; 32: 1299-1304.

[9] Li Y, Zhao ZX, Xu CH, Zhou ZQ, Zhu Z and You TG. HMGA2 induces transcription factor Slug expression to promote epithelial-to-mesenchymal transition and contributes to colon cancer progression. Cancer Lett 2014; 355: 130-140.

[10] Karimi Roshan M, Soltani A, Soleimani A, Rezaie Kahkhaie K, Afshari AR and Soukhtanloo M. Role of AKT and mTOR signaling pathways in the induction of epithelial-mesenchymal transition (EMT) process. Biochimie 2019; 165: 229-234.

[11] Dubey AR, Kinger S, Jagtap YA, Patwa SM, Kumar P, Singh S, Kumar A, Kumar A and Mishra A. Proteasome based molecular strategies against improper cellular proliferation. Cell Physiol Biochem 2021; 55: 120-143.

[12] Peris-Moreno D, Malige M, Claustre A, Armani A, Coudy-Gandilhon C, Deval C, Béchet D, Fafournoux P, Sandri M, Combaret L, Taillandier D and Polge C. UBE2L3, a partner of MuRF1/TRIM63, is involved in the degradation of myofibrillar actin and myosin. Cells 2021; 10: 1974.

[13] Yi SA, Kim GW, Yoo J, Han JW and Kwon SH. HP1γ sensitizes cervical cancer cells to cisplatin through the suppression of UBE2L3. Int J Mol Sci 2020; 21: 5976.

[14] Yu SJ, Yu HH, Zhang YF, Liu C, Zhang WL and Zhang YY. Long non-coding RNA LINC01116 acts as an oncogene in prostate cancer cells through regulation of miR-744-5p/UBE2L3 axis. Cancer Cell Int 2021; 21: 168.

[15] Liu Y, Song C, Ni HL, Jiao WJ, Gan WJ, Dong XQ, Liu JB, Zhu LG, Zhai XJ, Hu ZB and Li JM. UBE2L3, a susceptibility gene that plays oncogenic role in hepatitis B-related hepatocellular carcinoma. J Viral Hepat 2018; 25: 1363-1371.

[16] Ma XJ, Zhao JJ, Yang F, Liu HT and Qi WB. Ubiquitin conjugating enzyme E2 L3 promoted tumor growth of NSCLC through accelerating p27kip1 ubiquitination and degradation. Oncotarget 2017; 8: 84193-84203.

[17] Saw SPL, Ong BH, Chua KLM, Takano A and Tan DSW. Revisiting neoadjuvant therapy in non-small-cell lung cancer. Lancet Oncol 2021; 22: e501-e516.

[18] Denisenko TV, Budkevich IN and Zhivotovsky B. Cell death-based treatment of lung adenocarcinoma. Cell Death Dis 2018; 9: 117.

[19] Shao B, Bjaanæs MM, Helland Å, Schütte C and Conrad T. EMT network-based feature se-

lection improves prognosis prediction in lung adenocarcinoma. PLoS One 2019; 14: e0204186.
[20] Banerjee P, Xiao GY, Tan X, Zheng VJ, Shi L, Rabassedas MNB, Guo HF, Liu X, Yu J, Diao L, Wang J, Russell WK, Roszik J, Creighton CJ and Kurie JM. The EMT activator ZEB1 accelerates endosomal trafficking to establish a polarity axis in lung adenocarcinoma cells. Nat Commun 2021; 12: 6354.
[21] Zhang YF, Sun LZ, Gao X, Guo AN, Diao Y and Zhao Y. RNF43 ubiquitinates and degrades phosphorylated E-cadherin by c-Src to facilitate epithelial-mesenchymal transition in lung adenocarcinoma. BMC Cancer 2019; 19: 670.
[22] Becker KF, Rosivatz E, Blechschmidt K, Kremmer E, Sarbia M and Höfler H. Analysis of the E-cadherin repressor Snail in primary human cancers. Cells Tissues Organs 2007; 185: 204-212.
[23] Bai L, Yu ZB, Zhang JW, Yuan S, Liao C, Jeyabal PV, Rubio V, Chen HR, Li YF and Shi ZZ. OLA1 contributes to epithelial-mesenchymal transition in lung cancer by modulating the GSK3β/snail/E-cadherin signaling. Oncotarget 2016; 7: 10402-10413.
[24] Lin JT, Song T, Li C and Mao WF. GSK-3β in DNA repair, apoptosis, and resistance of chemotherapy, radiotherapy of cancer. Biochim Biophys Acta Mol Cell Res 2020; 1867: 118659.
[25] Duda P, Akula SM, Abrams SL, Steelman LS, Martelli AM, Cocco L, Ratti S, Candido S, Libra M, Montalto G, Cervello M, Gizak A, Rakus D and McCubrey JA. Targeting GSK3 and associated signaling pathways involved in cancer. Cells 2020; 9: 1110.
[26] Kazi A, Xiang S, Yang H, Delitto D, Trevino J, Jiang RHY, Ayaz M, Lawrence HR, Kennedy P and Sebti SM. GSK3 suppression up-regulates β-catenin and c-Myc to abrogate KRas-dependent tumors. Nat Commun 2018; 9: 5154.
[27] Ren JL, Liu TT, Han Y, Wang QZ, Chen YZ, Li G and Jiang LH. GSK-3β inhibits autophagy and enhances radiosensitivity in non-small cell lung cancer. Diagn Pathol 2018; 13: 33.
[28] Zeng J, Liu D, Qiu ZX, Huang Y, Chen BJ, Wang L, Xu H, Huang N, Liu LX and Li WM. GSK3β overexpression indicates poor prognosis and its inhibition reduces cell proliferation and survival of non-small cell lung cancer cells. PLoS One 2014; 9: e91231.
[29] Tao NN, Zhang ZZ, Ren JH, Zhang J, Zhou YJ, Wai Wong VK, Kwan Law BY, Cheng ST, Zhou HZ, Chen WX, Xu HM and Chen J. Overexpression of ubiquitin-conjugating enzyme E2 L3 in hepatocellular carcinoma potentiates apoptosis evasion by inhibiting the GSK3β/p65 pathway. Cancer Lett 2020; 481: 1-14.
[30] Liu Y, Zhou H, Zhu R, Ding F, Li Y, Cao X and Liu Z. SPSB3 targets SNAIL for degradation in GSK-3β phosphorylation-dependent manner and regulates metastasis. Oncogene 2018; 37: 768-776.
[31] Xu Y, Lee SH, Kim HS, Kim NH, Piao S, Park SH, Jung YS, Yook JI, Park BJ and Ha NC. Role of CK1 in GSK3beta-mediated phosphorylation and degradation of Snail. Oncogene 2010; 29: 3124-3133.